Deformation-tolerant Colour-array for Positioning, Measurement and Indoor Navigation

Zoltán Fazekas, Alexandros Soumelidis

Systems and Control Laboratory
MTA SZTAKI Institute for Computer Science and Control,
Budapest, Hungary

Abstract. Position-encoding colour-arrays, which are reasonably robust against deformations that are customary in vision-based measurements, for example, against deformations encountered in reflection-based corneal topography, are proposed and compared to more conventional position-encoding colour-arrays. The generation of the deformation-tolerant colour-arrays is outlined, and their application in corneal measurements is motivated. Finally, a pertinent positioning method is sketched.

Keywords: Colour-coding, positioning, indoor navigation, optical measurements, corneal measurements.

1 Introduction

To be sure about one's *ego-position in space* is fairly important, as anyone who had ever moved in a pitch dark room (spotted with awkwardly shaped obstacles all around), or had ever driven a car on unmarked roads in cold, foggy winter mornings (without any GPS support, of course) can passionately testify to this statement. People – including blind people – need some *natural or artificial reference* to feel comfortable in space. Similarly, a model-car equipped with a camera in an indoor environment carrying out some prescribed spatial manoeuvre, or some more practical mission for that matter, *needs some reference points in space*, be these points generally available in such environments, or specifically placed there for navigational purposes.

Static reference points that are usually available indoor environments include corners, fixed lighting equipments; less static reference objects – that could still be used for orienting a model-car – include tables, desks, chairs and beds. However, such objects may be hard to detect and identify in real-time. Therefore, fairly simple objects specifically designed for navigational purposes – i.e., *markers* – are often used in indoor navigation. For example, the *circular markers with bar-code-like rings* suggested in [2] fall into this latter type of reference objects.

Position-encoding colour-arrays with advantageous features were proposed in [1]. Firstly, only a few colours were used for generating the colour-array. Secondly, the array was generated in a way that ensured that each *cross-shaped neighbourhood* –

comprising one central cell and four neighbouring cells – appearing in it was unique, i.e., *no neighbourhood was repeated* in the generated colour-pattern. To make the pattern more practical, a further restriction was imposed on it: not only the cross-shaped neighbourhood itself was not to be repeated, but *neither were its rotated versions*. The rotations considered in [1] were of 90˚, 180˚ and 270˚.

Such a position-encoding colour-array was used in the *reflection-based measurement of specular surfaces* presented in [5].

2 Generation of the position-encoding colour-array

We implemented and used the *location-identification technique* – based on the aforementioned position-encoding colour-arrays – in a *corneal measurement system* described in [3] and [4].

Firstly, *our implementation differed* from the originally proposed one *only slightly*; namely, we considered 3-by-3 neighbourhoods – each comprising the central cell and eight neighbouring cells around it – instead of the originally proposed cross-shaped neighbourhoods, and we used constraints – similar to the original ones – posed on these 3-by-3 neighbourhoods.

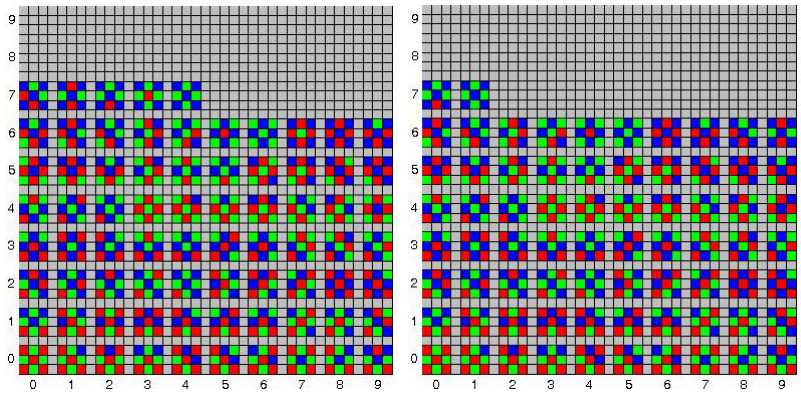

Fig. 1. The set of 3-by-3 coloured neighbourhoods available for the generation of position-encoding colour-arrays using red, green and blue. The neighbourhoods identical to ones after a rotation of 90˚, 180˚ or 270˚ have been removed from the set (a). The set neighbourhoods used for the generation colour-arrays; in this case, however, the neighbourhoods identical to ones either after a rotation of 90˚, 180˚ or 270˚, or after a quasi-rotation of 45˚, 135˚, 225˚ and 315˚ have been removed from the set (b).

Fig. 1a shows the *set of permissible ■-shaped neighbourhoods* (for colours red, green and blue), which can be used for the mentioned colour-pattern generation while observing its rotation constraints. As an example, *a 9-by-9-cell colour-array*, generated using the colour-neighbourhoods in Fig. 1a, is shown in Fig. 2a. The same colour-array presented as overlapping neighbourhoods is shown in Fig. 2b.

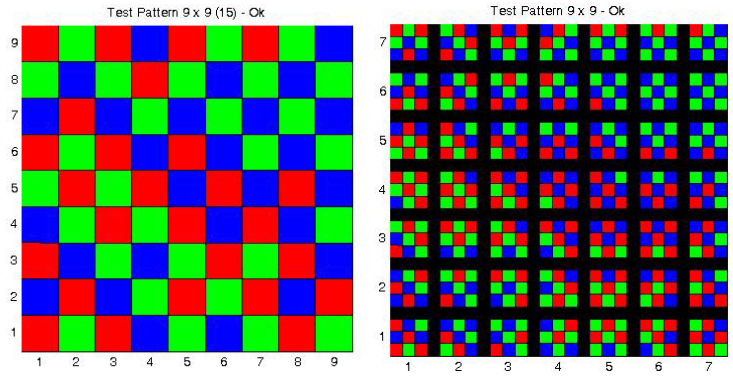

(a) (b)

Fig. 2. A three-colour (red, green and blue) position-encoding colour-array using the ■-shaped neighbourhoods of Fig. 1a (a). The same colour-array represented with overlapping neighbourhoods (b).

The *number of permissible neighbourhoods* – in case of three colours – is not very large, namely 68. It means that one *might* – or for that matter might not! – *be able* to create *a colour-square of 24-by-24 cells* by using each permissible neighbourhood at most once.

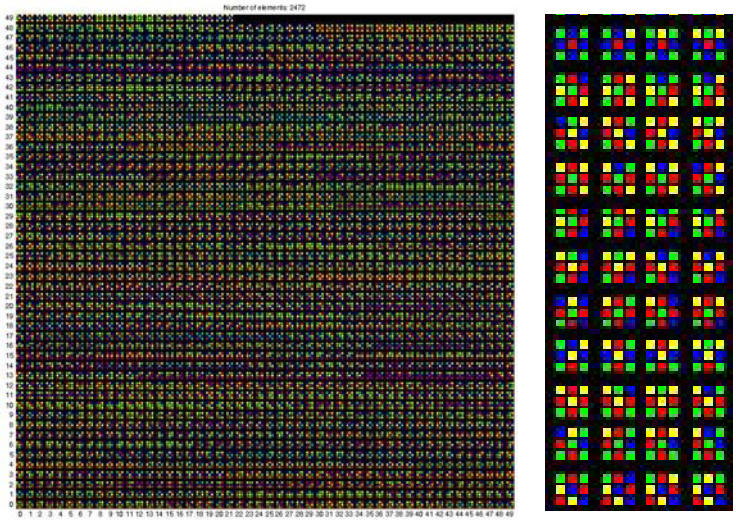

(a) (b)

Fig. 3. The set of 3-by-3 coloured neighbourhoods available for the generation of position-encoding colour-arrays using red, green, blue and yellow. The neighbourhoods identical to ones after a rotation of 90˚, 180˚ or 270˚ have been removed from the set (a). A more visible subset of the mentioned set (b).

In order to encode position within a *larger array of cells*, one has to *increase the number of colours* used. Fig. 3a shows the set of permissible neighbourhoods for four colours, namely for red, green, blue and yellow. These colour-neighbourhoods can be used for the colour-pattern generation while observing the rotation constraints.

As there are *quite a few of such neighbourhoods*, they do not show up very clearly in printing. Therefore, a small subset of the set is repeated in Fig. 3b to better illustrate the concept.

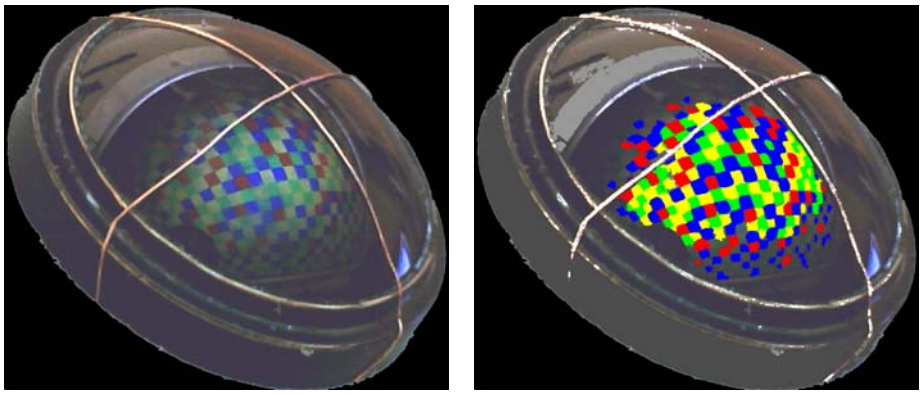

(a) (b)

Fig. 4. An artificial test-cornea reflecting a position-encoding colour-array displayed by a monitor (a). The same image with the colour-pattern's original colours restored (b).

When working with *corneal images* in order to determine the optical characteristics of the cornea, *pattern-deformations* similar to that appearing in Fig. 4a occur. The colour-array that is being reflected there is presented in Fig. 8a. The deformed colour-pattern with the original colours already restored is shown in Fig. 4b.

Clearly, the *regular neighbourhood structure* characterising the original colour-array, is lost with the *imperfectly segmented*, *deformed blobs* appearing in Fig. 4b. A detail of the figure is shown enlarged in Fig. 5a for better visibility.

For example, the *green blobs* – marked with the dashed circle – correspond to two *diagonally connected*, green squares within the position-encoding colour-pattern. The blobs are *connected in a more profound way*.

Based on the observation that the neighbourhood structure might be affected by imperfect segmentation, and aiming for unique location-identification, we used *a stronger constraint* – based on generalised rotation – *on colour-neighbourhoods*.

Colour-neighbourhoods, which can be reproduced applying this more general rotation to a neighbourhood that is already in the permissible set, are not included in the permissible set. The *generalised rotation* used was the *circular shift of the peripheral cells* of the 3-by-3 neighbourhood. Fig. 1b shows the set of permissible 3-colour-neighbourhoods under this stronger constraint.

Comparing the sets of neighbourhoods shown in Figs. 1a and 1b – considering the neighbourhoods from left to right and from bottom up – the *first difference one can*

spot is in row 4 and column 9. The colour-neighbourhood in this position is shown enlarged in Fig. 6a.

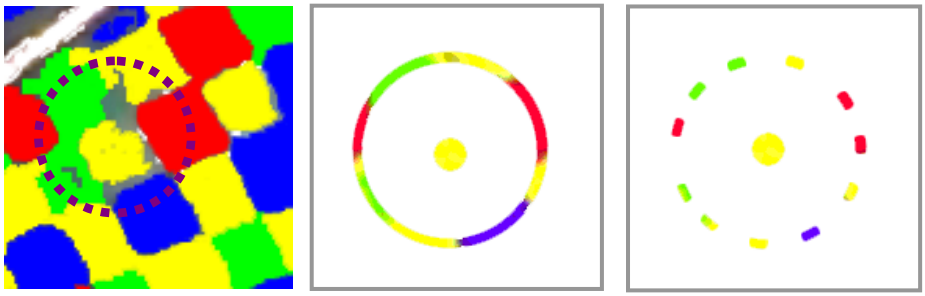

(a) (b) (c)

Fig. 5. A detail of the colour-restored reflection shown in Fig. 4b with a dashed circle overlaid on it (a). The colours found along the circle and in its centre (b). The sampled version of the circle (c).

Indeed, this *neighbourhood cannot be accepted* in the permissible set shown in Fig. 1b, as it is a *circular-shifted version of another neighbourhood* already in the set, namely, of the one appearing in position row 0, column 7. The latter colour-neighbourhood is shown in Fig. 6b. The set of permissible – under this stronger constraint – neighbourhoods for four colours, namely for red, green, blue and yellow, is shown in Fig. 7a. Again, as there are quite a few of such neighbourhoods and they do not show up clearly in print, a small subset is repeated in Fig. 7b.

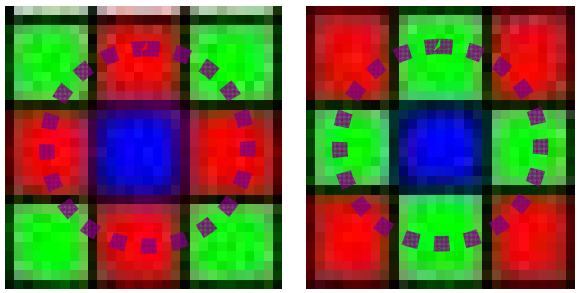

(a) (b)

Fig. 6. The first colour-neighbourhood of the set shown in Fig. 1a that could not be included into the set shown in Fig. 1b.

In Fig. 8a, *a four-colour* (red, green, blue and yellow) *position-encoding colour-array* generated under the mentioned *stronger constraints* is shown. The same colour-array presented as overlapping neighbourhoods is shown in Fig. 8b.

The i*mplementation* of the colour-array's generation is based on *complete search*, so in case of bigger colour-arrays, the *time required to fill up the array* with unique neighbourhoods – observing also the rotation-related constraints stated above – may

be *rather long*. It is because of the many *backtracking steps* required after reaching unacceptable neighbourhood-constellations in the array.

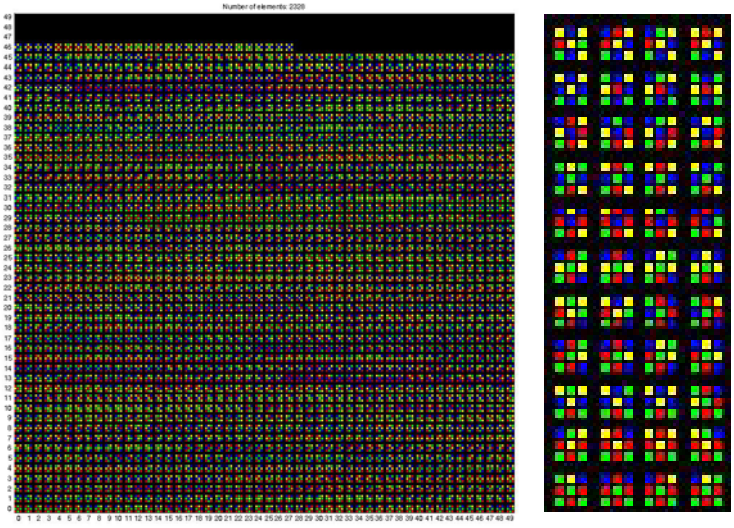

(a) (b)

Fig. 7. The set of 3-by-3 coloured neighbourhoods available for the generation of the 4-colour-arrays using red, green, blue and yellow. The neighbourhoods identical to ones either after a rotation of 90˚, 180˚ or 270˚, or after a quasi-rotation of 45˚, 135˚, 225˚ and 315˚ have been removed from the set (a). A more visible subset of the set (b).

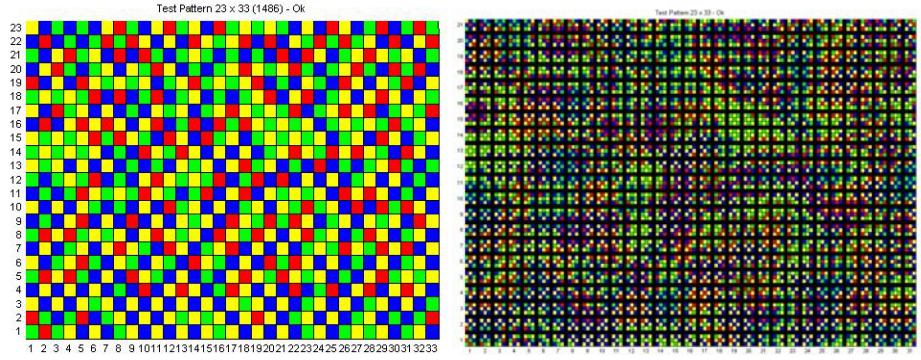

(a) (b)

Fig. 8. A four-colour (red, green and blue) position-encoding colour-array using the ■-shaped neighbourhoods of Fig. 7a (a). The same colour-array represented with overlapping neighbourhoods (b).

The *identification of the location on a distorted* – in the concrete case given above, even reflected – *image* of the colour-array is carried out in the manner suggested by Figs. 5a-c.

Samples from the *colour-restored image* at *discrete points of circles* of different sizes – and, if necessary, of ellipses of different parameters – are taken and checked whether they are likely to represent – and thus locate – a *valid colour-neighbourhood*, as is the case in Fig. 5c. Note that some tolerance can and should be incorporated here as a means of filtering.

Using this location-identification approach in *corneal topography*, the *discrete mathematical mapping* between the *original grid* – corresponding to the colour-array being reflected – and the *distorted grid* – recorded by one or more calibrated camera – can be determined. Then, from this discrete mapping, a smooth, *continuous mapping* can be constructed. Using the continuous mapping, the *corneal surface* can be geometrically *reconstructed* as described in some detail in [3] and [4].

3 Conclusions

We presented *planar deformation-tolerant colour-arrays* for positioning, measurement and indoor navigation purposes, motivated their use and discussed their advantages. We explained its colour-array generation process. The location-identification approach based on such colour-arrays can be used in many positioning, measurement and navigational tasks, particularly in indoor situation and when *planar navigation* is sufficient. As a concrete application example, we mentioned *corneal topography*. In that case, the discrete mapping between the original and the distorted grids can be sought using this location-identification technique.

References

1 Griffin, P. M., Narasimhan, S. and Yee, S. R.: Generation of uniquely encoded light patterns for range data acquisition. Pattern Recognition, vol. 25, no. 6, pp. 609-616, (1992).

2. Fazekas, Z., Soumelidis, A., Bokor, J., Péni, T. and Rödönyi, G.: An inexpensive indoor self-positioning system for mobile platforms with web-camera. Proceedings of Joint Hungarian-Austrian Conference on Image Processing and Pattern Recognition, Veszprém, Hungary, pp. 33-40, (2005)

3. Fazekas, Z., Soumelidis, A., Bódis-Szomorú, A.. and Schipp, F. Specular surface reconstruction for multi-camera corneal topographer arrangements, Proceedings of 30th Annual International IEEE EMBS Conference, pp. 2254-2257, Vancouver, Canada, (2008).

4. Somelidis, A., Fazekas, Z., Bódis-Szomorú, A., Schipp, F., Csákány, B. and Németh, J.: Specular surface reconstruction method for multi-camera corneal topographer, In: Recent advances in biomedical engineering, G. R. Naik (ed.), In-Teh, Vukovar, Croatia, pp. 639-660, (2009).

5. Bonfort, T. and Sturm, P.: Voxel carving for specular surfaces. Proceedings of the 9th IEEE Conference on Computer Vision, Vol. 2. IEEE. (2003).